energies

Article

Investigation and Analysis of R463A as an Alternative Refrigerant to R404A with Lower Global Warming Potential

Piyanut Saengsikhiao [1], Juntakan Taweekun [2,*], Kittinan Maliwan [2], Somchai Sae-ung [2] and Thanansak Theppaya [2]

1 Energy Technology Program, Faculty of Engineering, Prince of Songkla University, Songkhla 90112, Thailand; nacky_pik@hotmail.com
2 Department of Mechanical Engineering, Faculty of Engineering, Prince of Songkla University, Songkhla 90112, Thailand; kittinan.m@psu.ac.th (K.M.); sasomchai@gmail.com (S.S-u.); tthanand@eng.psu.ac.th (T.T.)
* Correspondence: jantakan.t@psu.ac.th or juntakan2016@gmail.com

Received: 21 February 2020; Accepted: 18 March 2020; Published: 23 March 2020

Abstract: This research presents the development of R463A refrigerant, a nonflammable refrigerant that was retrofitted to replace R404A. R463A is primarily composed of hydrofluorocarbons/hydrocarbons/carbon dioxide (HFCs/HCs/CO_2), and has global-warming potential (GWP) of 1494. It is a nonazeotropic mixture of R32 (36%), R125 (30%), R134a (14%), R1234yf (14%), and R744 (6%). R463A is composed of polyol ester oil (POE), and it is classified as a Class A1 incombustible and nontoxic refrigerant. R463A has a higher cooling capacity (Qe) than that of R404A, as it is composed of hydrofluorocarbons (HFCs) R32 and carbon dioxide (CO_2) R744, and has lower GWP than that of R404A due to the use of hydrofluoroolefins (HFOs) from R1234yf. The results of this research showed that R463A can be retrofitted to replace R404A due to its composition of POE, Class A1 incombustibility, and lower toxicity. The properties of R463A and R404A, as analyzed using national institute of standards and technology (NIST) reference fluid thermodynamic and transport properties database (REFPROP) software and NIST vapor compression cycle model accounting for refrigerant thermodynamic and transport properties (CYCLE_D-HX) software, are in accordance with the CAN/ANSI/AHRI540 standards of the Air-Conditioning, Heating, and Refrigeration Institute (AHRI). The normal boiling point of R463A was found to be higher than that of R404A by 23%, with a higher cooling capacity and a 63% lower GWP value than that of R404A. The critical pressure and temperature of R463A were found to be higher than those of R404A; it can be used in a high-ambient-temperature environment, has higher refrigerant and heat-rejection effects, and has lower GWP than that of R404A by 52% due to the HFOs from the R1234yf component. The cooling coefficient of performance (COPc) of R463A was found to be higher than that of R404A by 10% under low-temperature applications. R463A is another refrigerant option that is composed of 7% carbon dioxide (CO_2), and is consistent with the evolution of fourth-generation refrigerants that contain a mixture of HFCs, HFOs, HCs, and natural refrigerants, which are required to produce a low-GWP, zero-ozone-depletion-potential (ODP), high-capacity, low-operating-pressure, and nontoxic refrigerant.

Keywords: R463A refrigerant; refrigeration system; energy technology; environmentally friendly

1. Introduction

Energy use in Thailand's business sector is ranked second among overall energy users in the country, and is thus being targeted for energy-saving options [1]. The number of convenience stores in Thailand numbered to more than 20,000 locations in 2019, and this continuously increases on an annual basis. The majority are open 24 h per day, so the retail sector is the fourth largest consumer of energy in the business sector, consuming more energy than residences do [2]. The components that contribute to energy consumption of convenience stores in Thailand, ranked from highest to lowest, are refrigeration systems, air-conditioning systems, electrical equipment, and lighting [3,4]. However, proportions of energy use in convenience stores in Taiwan were previously ranked as shown in Figure 1 below [5]. The best options for reducing energy consumption in convenience stores in Thailand are high energy efficiency and an efficient energy-management system. A good example of energy savings in refrigeration systems is shown in Figure 2 below [6]. Energy savings in refrigeration systems can be achieved through decreased power consumption of the compressor, as this is the component that utilizes the most energy.

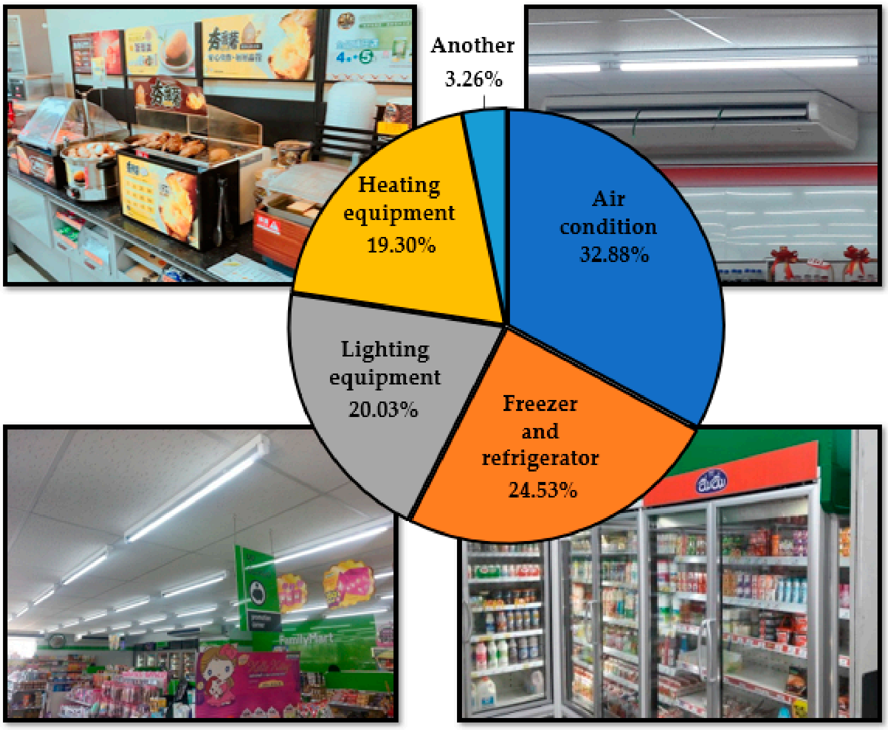

Figure 1. Proportions of energy use in Taiwanese convenience stores [5].

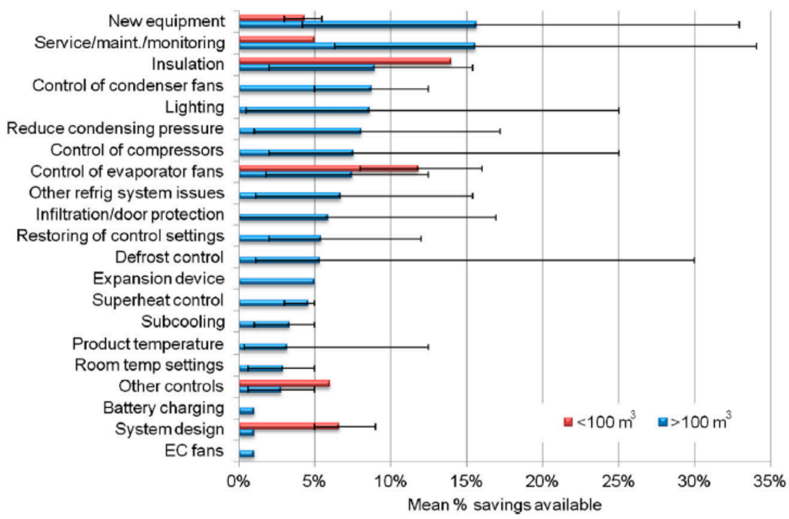

Figure 2. Examples of energy savings in refrigeration systems [6].

Refrigerant trends in Thailand have shown improvements in increasing energy efficiency and decreasing global-warming potential (GWP), as shown in Figure 3 [7,8], which is related to the hydrofluorocarbon (HFC) phase-down schedule, as shown in Figure 4 [9]. First- and second-generation refrigerants were composed of natural refrigerants and hydrocarbons (HCs), both of which do not impact the environment, have low GWP, and zero ozone-depletion potential (ODP) [10–12]. R744 operates under high pressure, and is highly toxic and flammable (Figure 5) [13–15]. Following the second generation, third-generation refrigerants were composed of chlorofluorocarbons (CFCs) [16–18] and hydrochlorofluorocarbon (HCFCs) [19–21], which are easy to use, can operate under low pressure, and are nontoxic. However, they have high GWP and ODP, contributing to ozone depletion and global warming. Therefore, the development of refrigerants has significantly decreased ODP and GWP. Moreover, third-generation refrigerants, CFCs and HCHCs, were further developed into hydrofluorocarbon (HFC) refrigerants that still possessed low GWP and zero-ODP [22–24]. Fourth-generation refrigerants are mainly hydrofluoroolefins (HFOs) with low GWP and low capacity [25–27]. Therefore, they are refrigerants that are mixed with HFCs [28–30], HFOs [31–33], and HCs [34–36]. Natural refrigerants are low-GWP, zero-ODP, high-capacity, low-pressure, and nontoxic [37–39].

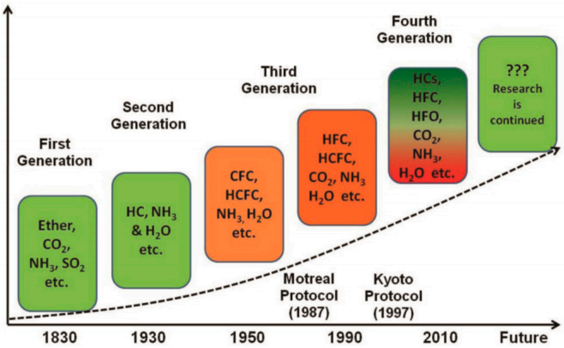

Figure 3. Evolution of refrigerants [7].

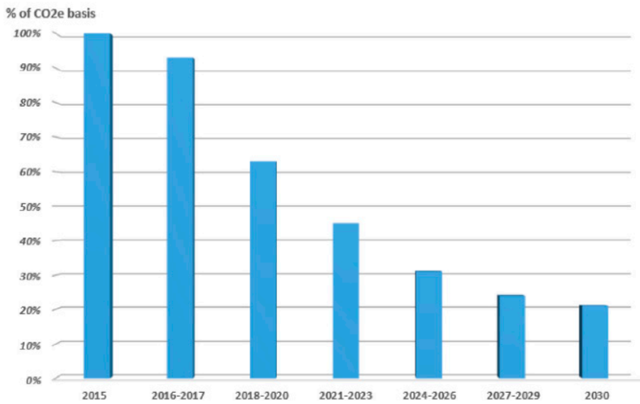

Figure 4. Hydrofluorocarbon (HFC) phase-down schedule (Co2e %) [9].

Refrigerants need to be low-GWP, zero-ODP, high-capacity, low-pressure, and nontoxic, and should thus be mixed with HCs and HFOs; however, current refrigerants are still highly flammable and have low capacity. An alternative is to incorporate other HFCs. R32 is low-GWP, zero-ODP, high-capacity, and nontoxic, but operates under high pressure and is not flammable, which is in contrast to R134A, which possesses highly similar properties but can operate under low pressure and has low capacity. Systems that operate with R22 [40], R407C [41], R417A [42], R422A [43], R422D [44], R424A [45], R427A [46], and R453A [47] were developed as an alternative to R22 and mixed with HCs and HFCs, as shown in Tables 1 and 2. Systems that operate with R134A [48], R450A [49], R456A [50], R513A [51], and R515A [50] were developed as an alternative to R134A, and mixed with HCs, HFCs, and HFOs, as shown in Table 3. The fourth-generation R404A was the basis for this research, and it is currently the most used refrigerant, as shown in Figure 6. R404A is an azeotropic blend of 143a/125/134a with zero ODP, and is nonflammable, nontoxic, and operates under low pressure, but has a GWP of 3922 [52]. R407A [53], R407F [54], R407H [55], R410A [56], R442A [57], R448A [58], R449A [59], R452A [60], R453A [57], and R463A [50] were developed to be retrofitted to replace R404A, and are mixed with HCs, HFOs, R134A, and R32. This is similar to the refrigerant that was developed for R22 and R134A but does not include R463A, which is being presented as a refrigerant for comparative purposes in this research as it is composed of R744 (carbon dioxide), which is a natural refrigerant similar to R445A [61] and R455A [62]. These conform to the refrigerant-development trend and are an alternate option that can be mixed with HFC. The refrigerant proportion that was mixed with R125 was more or less similar to that of the R32 mixture, and it also possesses Class A1 nonflammability property.

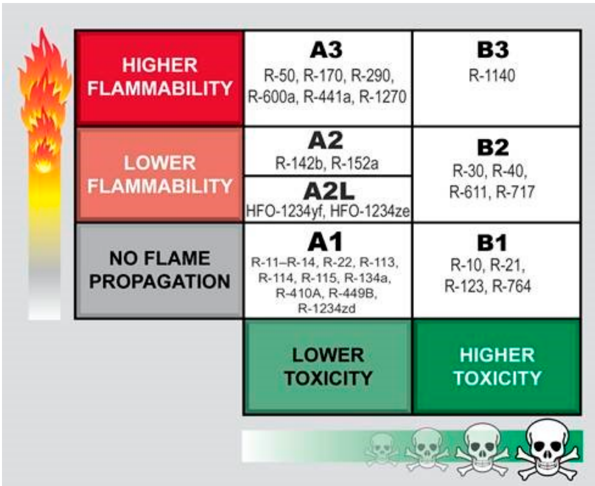

Figure 5. Refrigerant classification.

Table 1. Properties of 22, R407C, R417A, and R422A. Note: ODP, ozone-depletion potential; GWP, global-warming potential.

Refrigerant	R22 [40]	R407C [41]	R417A [42]	R422A [43]
Composition	R22	R125/R134a/R32	R125/R134a/R600	R125/R134a/R600a
Mass percentage	100	25/52/23	46.6/60/3.4	85.1/11.5/3.4
Boiling point (°C)	−40.8	−43.6	−39.1	−46.8
Critical pressure (kPa)	4990	4620	4036	3665
Critical temperature (°C)	96.1	86.74	87	71.7
ODP	0.055	0	0	0
GWP	1600	1526	1950	2530
Class	A1	A1	A1	A1
Lubricant type	MO	MO	MO/AB/POE	MO/AB/POE

Table 2. Properties of R422D, R424A, R427A, and R453A.

Refrigerant	R422D [44]	R424A [45]	R427A [46]	R453A [47]
Composition	R125/R134a/ R600a	R125/R134a/R600/ R600a/R601a	R125/R134a/ R143a/R32	R125/R134a/R32/ R227ea/R600a/R601a
Mass percentage	62.1/31.5/3.4	50.5/47/1/0.9/0.9	25/50/10/15	20/53.8/20/5/0.6/0.6
Boiling point (°C)	−43.5	−38.7	−42.7	−60.13
Critical pressure (kPa)	3795	4040	4330	4530
Critical temperature (°C)	79.6	88.8	86.8	87.9
ODP	0	0	0	0
GWP	2330	2440	2138	1765
Class	A1	A1	A1	A1
Lubricant type	MO/AB/POE	MO/AB/POE	MO/POE	MO/AB/POE

Table 3. Properties of R134A, R450A, R456A, R513A and R515A.

Refrigerant	R134A [48]	R450A [49]	R456A [50]	R513A [51]	R515A [50]
Composition	R134A	R134A/ R12354ze(E)	R134a/R32/R1234ze (E)	R134A/ R1234yf	R227ea/ R1234ze
Mass percentage	100	42/58	45/6/49	44/56	12/88
Boiling point (°C)	−26.07	−23.5	−30.75	−28.3	−18.75
Critical pressure (kPa)	4060	3814	4175	3700	3555
Critical temperature (°C)	101.06	105.87	102.65	97.7	108.65
ODP	0	0	0	0	0
GWP	1430	547	687	570	387
Class	A1	A1	A1	A1	A1
Lubricant type	POE	POE	POE	POE	POE

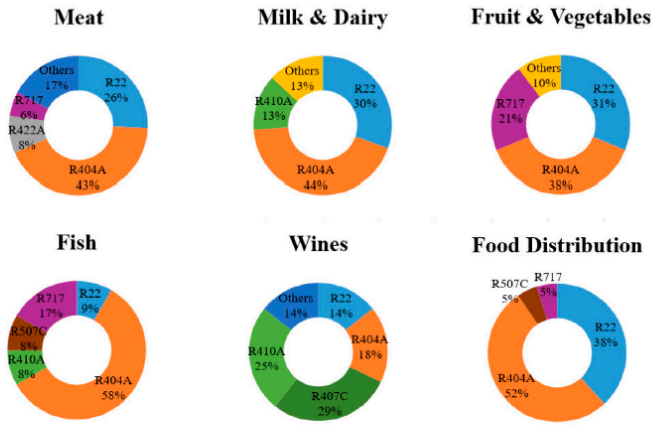

Figure 6. Top refrigerants in food industry [9].

2. Materials and Methods

The R463A refrigerant is a nonflammable refrigerant that was developed to be retrofitted to R404A. The hydrofluorocarbons/hydrocarbons/carbon dioxide (HFCs/HCs/CO_2) of R463A (GWP = 1494) are an azeotropic mixture of R32 (36%), R125 (30%), R134a (14%), R1234yf (14%), and R744 (6%) [50]. R463A is composed of polyol ester oil (POE), and classified as a Class A1 incombustible and nontoxic refrigerant. The components of R463A are consistent with R445A, which is a mixture of R1234z3 (85%), R134 (9%), and R744 (6%) (HFOs/HFCs/CO_2) [61], and also consistent with the components of R455A, which is a mixture of R1234yf (75.5%), R32 (21.5%), and R744 (3%) (HFOs/HFCs/CO_2) [62]. R463A, R445A, and R455A have higher cooling capacity (Qe) than that of R404A due to the hydrofluorocarbons (HFCs) of R32 [63–65] and carbon dioxide (CO_2) of R744 in their components [66–68], and a lower global-warming potential (GWP) than that of R404A due to the presence of hydrofluoroolefins (HFOs) from R1234yf [57,58,69]. The P–H diagram of R463A and R404A is shown in Figure 7. Both refrigerants conformed to the use of the REFPROP [59,60,70] and CYCLE_D-HX [61,62,71] software, and are in accordance with the CAN/ANSI/AHRI540 Air-Conditioning, Heating, and Refrigeration Institute (AHRI) standards, as shown in Table 4 [34,63,64].

Table 4. Medium back pressure standard testing for refrigeration systems [34,63,64].

Temperature Point	Air Conditioning and Heat Pump		Refrigeration		
	Heating	Cooling	Low	Medium	High
Suction dew point (°C)	−15.0	10.0	−31.5	−6.5	7.0
Discharge dew point (°C)	35.0	46.0	40.5	43.5	54.5
Suction return gas temperature (°C)	−4.0	21.0	4.5	18.5	18.5
Superheat (K)	11.0	11.0	11.0	11.0	11.0
Subcooling (K)	0.0	0.0	0.0	0.0	0.0

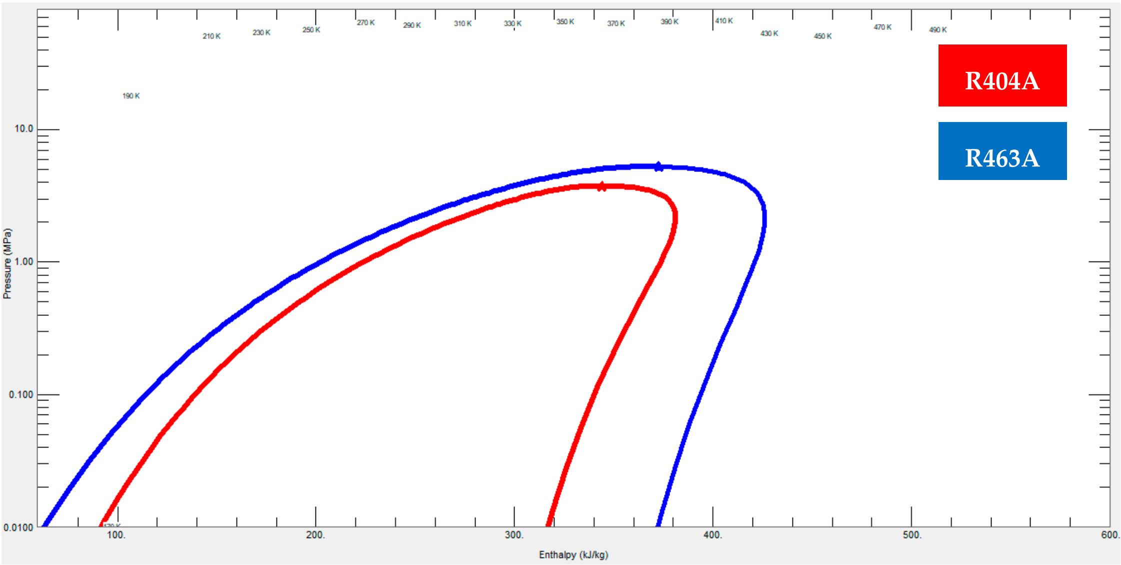

Figure 7. Properties of R463A obtained from REFPROP.

The properties of R463A, R404A, and other refrigerants, summarized in Tables 5–8, conform to the use of REFPROP [59,60,70] and CYCLE_D-HX [61,62,71] software, as stipulated by the National Institute of Standards and Technology (NIST) [65–67], and are in accordance with the CAN/ANSI/AHRI540 Air-Conditioning, Heating, and Refrigeration Institute (AHRI) standards, as shown in Table 4 [34,63,64]. Both software programs can predefine mixtures and create new refrigerant mixtures. REFPROP can display results related to refrigerant properties under various conditions, and the CYCLE_D-HX software can also display results related to refrigerant cycles under various conditions. Results illustrated the relationship of all parameters for R407A, R407F, R407H, R410A, R442A, R448A, R449A, R450A, R452A, R453A, and R463A, such as GWP, boiling point, refrigerant effect, heat rejection, refrigerant work, evaporator pressure, high pressure, and cooling coefficient of performance (COPc), as shown in Tables 5–7.

Table 5. Properties of R404A, R407A, and R407F.

Condition	LT	MT	HT	LT	MT	HT	LT	MT	HT
Refrigerant		R404A [52]			R407A [53]			R407F [54]	
Composition		R125/R143/R134A			R125/R32/R134A			R125/R32/R134A	
Mass percentage		44/52/4			40/20/40			30/30/40	
Boiling point (°C) at 1 kPa		−46.6			−45.28			−46.33	
Critical pressure (kPa)		3728			4494			4754	
Critical temperature (°C)		72.1			82			82.6	
ODP		0			0			0	
GWP		3943			2107			1825	
Class		A1			A1			A1	
Lubricant type		POE			POE			POE	
Liquid density (kg/m^3) at 25 °C		1044.1			1145.1			1117.0	
Vapor density (kg/m^3) at 25 °C		65.27			49.74			45.1	
Cp liquid (kJ/kg.K) at 25 °C		1.542			1.520			1.570	
Cp vapor (kJ/kg.K) at 25 °C		1.221			0.829			1.180	
Liquid conductivity (mW/m.K) at 25 °C		62.71			81.90			89.71	
Vapor conductivity (mW/m.K) at 25 °C		17.00			13.14			14.51	
Qevap (kJ/kg)	83.66	139.02	N/A	119.21	126.89	114.83	192.46	184.93	170.29
Qcond (kJ/kg)	159.8	198.57	N/A	216.04	189.24	166.05	328.41	266.99	237.2
Work (kJ/kg)	76.14	59.55	N/A	96.83	62.35	51.22	135.95	82.06	66.91
COPc	1.099	2.335	N/A	1.231	2.035	2.242	1.416	2.254	2.545
Evaporator pressure (kPa)	183.30	477.3	N/A	140.90	392.80	676.2	149.50	414.40	714.30
Condenser pressure (kPa)	2197.50	2284.10	N/A	2103.40	2308.40	2961.2	2101.20	2323.80	2987.00
Evaporator temp glide (°C)	−0.4	−0.5	N/A	−3.4	−3.5	−3.1	−5.0	−4.7	−4.3
Condenser temp glide (°C)	0.3	0.3	N/A	4.1	3.9	3.3	4.2	4.0	3.4

Table 6. Properties of R407H, R410A, and R422A.

Condition	LT	MT	HT	LT	MT	HT	LT	MT	HT
Refrigerant		R407H [55]			R410A [56]			R442A [57]	
Composition		R125/R32/R134A			R125/R32			R125/R32/R1234A/R227ea/R152A	
Mass percentage		15/32.5/52.5			50/50			31/31/30/5/3	
Boiling point (°C)		−44.6			−51.6			−46.5	
Critical pressure (kPa)		4856			4811			4760	
Critical temperature (°C)		86.53			70.81			82.4	
ODP		0			0			0	
GWP		1400			1900			1888	
Class		A1			A1			A1	
Lubricant type		POE			POE			POE	
Liquid density (kg/m^3) at 25 °C		1111.2			1058.6			1108.5	
Vapor density (kg/m^3) at 25 °C		41.86			65.97			47.4	
Cp liquid (kJ/kg.K) at 25 °C		1.585			1.708			1.579	
Cp vapor (kJ/kg.K) at 25 °C		1.176			1.445			1.184	
Liquid conductivity (mW/m.K) at 25 °C		90.2			89.19			85.83	
Vapor conductivity (mW/m.K) at 25 °C		14.58			15.73			14.76	
Qevap (kJ/kg)	148.59	155.8	142.95	139.33	188.53	N/A	191.98	184.39	169.63
Qcond (kJ/kg)	263.52	229.56	203.59	248.17	271.65	N/A	328.25	266.68	236.71
Work (kJ/kg)	114.94	73.76	60.64	108.84	83.12	N/A	136.27	82.29	67.07
COPc	1.293	2.112	2.357	1.28	2.268	N/A	1.409	2.241	2.529
Evaporator pressure (kPa)	135.00	379.10	656.8	247.60	636.30	N/A	150.90	417.50	718.90
Condenser pressure (kPa)	2060.40	2265.80	2915.4	2844.50	3013.70	N/A	2118.90	2342.40	3008.20
Evaporator temp glide (°C)	−3.9	−4.1	−3.7	0.0	−0.1	N/A	−5.2	−4.9	−4.5
Condenser temp glide (°C)	4.7	4.5	3.9	0.1	0.1	N/A	4.4	4.2	3.6

Table 7. Properties of R448A, R449A, and R452A.

Condition	LT	MT	HT	LT	MT	HT	LT	MT	HT
Refrigerant		R448A [58]			R449A [59]			R452A [60]	
Composition		R125/R32/R134A/ R1234yf/R12354ze(E)			R125/R32/R134A/R1234yf			R125/R32/R1234yf	
Mass percentage		26/26/20/21/7			24.7/24.3/25.7/25.3			59/11/30	
Boiling point (°C)		−40.1			−45.95			−47.2	
Critical pressure (kPa)		4675			4662			4014	
Critical temperature (°C)		83.66			83.85			75.05	
ODP		0			0			0	
GWP		1273			1282			1945	
Class		A1			A1			A1	
Lubricant type		POE			POE			POE	
Liquid density (kg/m^3) at 25 °C		1092.3			1097.1			1125.5	
Vapor density (kg/m^3) at 25 °C		48.5			49.32			64.10	
Cp liquid (kJ/kg.K) at 25 °C		1.553			1.55			1.470	
Cp vapor (kJ/kg.K) at 25 °C		1.165			1.162			1.100	
Liquid conductivity (mW/m.K) at 25 °C		80.60			80.00			66.80	
Vapor conductivity (mW/m.K) at 25 °C		14.60			14.67			14.80	
Qevap (kJ/kg)	179.93	172.76	158.78	178.08	170.94	157.04	83.97	92.46	82.56
Qcond (kJ/kg)	305.77	249.11	221.17	301.63	245.91	218.33	159.88	141.82	122.68
Work (kJ/kg)	125.84	76.35	62.39	123.55	74.98	61.3	75.91	49.36	40.12
COPc	1.43	2.263	2.545	1.441	2.28	2.562	1.106	1.873	2.058
Evaporator pressure (kPa)	150.60	410.60	701.90	150.70	409.60	699.00	168.20	443.70	742
Condenser pressure (kPa)	2051.80	2265.90	2903.70	2027.80	2240.20	2871.90	2221.20	2423.00	3021.1
Evaporator temp glide (°C)	−4.9	−4.7	−4.4	−4.4	−4.3	−4	−1.9	−2.2	−2
Condenser temp glide (°C)	4.5	4.3	3.7	4.2	4.0	3.4	3.1	2.9	2.4

Table 8. Properties of R453A and R463A.

Condition	LT	MT	HT	LT	MT	HT
Refrigerant		R453A [57],			R463A [50]	
Composition		R125/R32/R134A/R227ea/ R600/R601A			R125/R32/R134A/R1234yf/R744	
Mass percentage		20/20/53.8/5/0.6/0.6			30/36/14/14/6	
Boiling point (°C)		−42.2			−60.13	
Critical pressure (kPa)		4530			5283	
Critical temperature (°C)		87.9			73.15	
ODP		0			0	
GWP		1765			1377	
Class		A1			A1	
Lubricant type		POE			POE	
Liquid density (kg/m^3) at 25 °C		1136			1051.4	
Vapor density (kg/m^3) at 25 °C		41.69			57.67	
Cp liquid (kj/kg.K) at 25 °C		1.5209			1.694	
Cp vapor (kj/kg.K) at 25 °C		1.337			1.256	
Liquid conductivity (mW/m.K) at 25 °C		83.30			87.16	
Vapor conductivity (mW/m.K) at 25 °C		15.72			15.47	
Qevap (kJ/kg)	184.91	178.36	165.49	194.65	186.07	168.25
Qcond (kJ/kg)	312	255.92	228.96	340.43	273.5	239.3
Work (kJ/kg)	127.56	77.56	63.47	145.78	87.43	71.05
COPc	1.45	2.3	2.607	1.335	2.128	2.368
Evaporator pressure (kPa)	121.00	342.10	595.7	209.10	554.10	934.70
Condenser pressure (kPa)	1808.70	2002.50	2584.3	2748.70	2988.10	3784.70
Evaporator temp glide (°C)	−5.2	−5.1	−4.7	−6	−6.1	−5.6
Condenser temp glide (°C)	5.0	4.8	4.2	6.5	6.2	4.9

3. Results and Discussion

The results of the boiling point, shown in Figure 8 below, indicate that the lowest normal boiling point of R463A was −60.13 °C, which was lower than that of R404A by 23%. This was due to hydrofluorocarbons (HFCs) R32 (36%) and carbon dioxide (CO_2) R744 (7%) in its composition, which were consistent with those of R445A and R455A. R445A [61] and R455A [68] displayed low boiling points of −49.15 and −52.0 °C, respectively, and are attractive as an alternative refrigerant with a lower GWP, to R134A and R404A [62], due to CO_2 R744 contents of 6% and 3%, respectively, in their compositions. R448A and R449A displayed the lowest GWP values at 1273 and 1282, respectively, due to the HFOs from R1234yf and R1234ze in their compositions [58,59], as shown in Figure 9. The GWP of R463A was found to be 1377, with a lower boiling point than that of R404A by 23%, even though the ratio of R1234yf in R463A was less than that in both R448A and R449A. However, the GWP of R463A was found to be slightly higher than that of R448A and R449A. The cost of R463A is also lower than that of R448A and R449A. Hydrofluorocarbons can also be combined with carbon dioxide (CO_2), which has a lower GWP and boiling point [54]. The lower boiling point and GWP are consistent with the evolution of the fourth-generation refrigerants that contain a mixture of HFCs, HFOs, HCs, and natural refrigerants, which are required to produce a low-GWP, zero-ODP, high-capacity, low-operating-pressure, and nontoxic refrigerant.

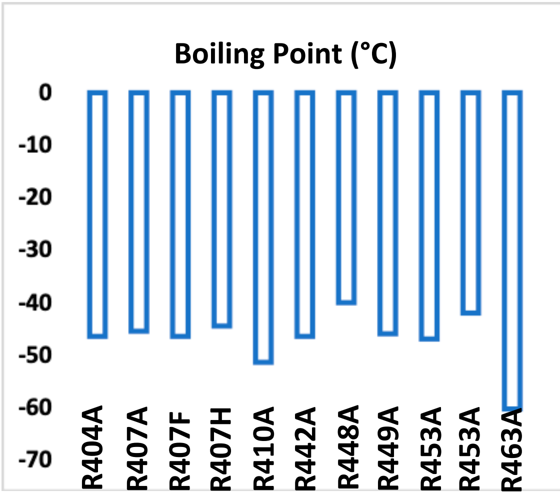

Figure 8. Normal boiling point of all refrigerants.

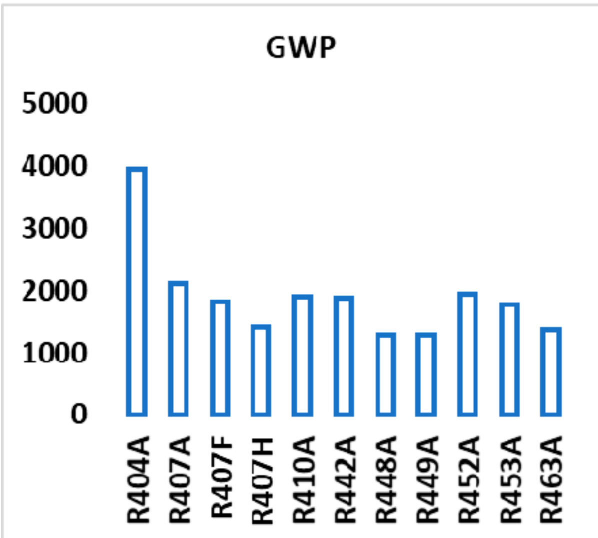

Figure 9. GWP of all refrigerants.

Results related to Cp liquid are shown in Figure 10, and they present the highest values for R410A and R463A at 1.708 and 1.694 kJ/kg.K, respectively, which are higher than those of R404A by 9.72% and 8.97% due to the HFCs and carbon dioxide (CO_2) from R744. This is consistent with boiling points of R410A and R463A; the highest boiling points were −51.6 and −60.3 °C due to the hydrofluorocarbons (HFCs) and carbon dioxide (CO_2) from R744. The 6% R744 in the composition of R463A affects the normal boiling point of R463A, which is higher than that of R410A by 14.5% even though R32 is in the composition of R410A 50%. The Cp result is consistent with that of liquid conductivity in Figure 11, but the effect of R32 is greater than the effect of R744 because the liquid conductivity of R32 is higher than that of R744. The boiling point, GWP, Cp, and liquid conductivity provide the basis to design the refrigerant. For the next steps, the Qevap, Qcond, work, evaporator pressure, and condenser pressure are considered.

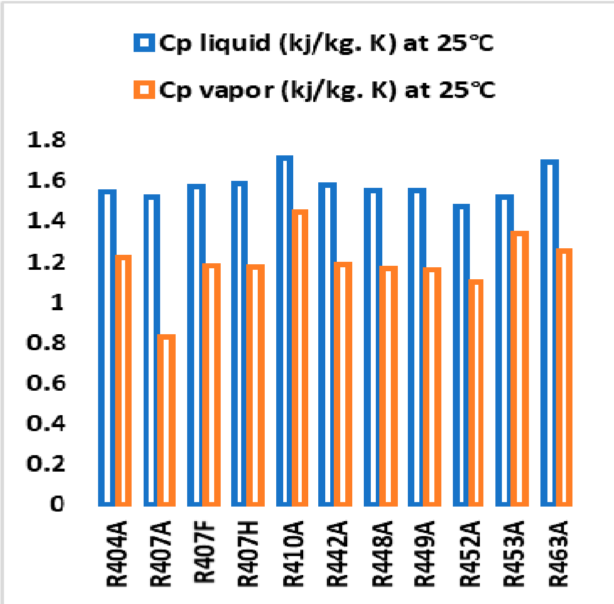

Figure 10. Cp liquid/vapor (kJ/kg.K).

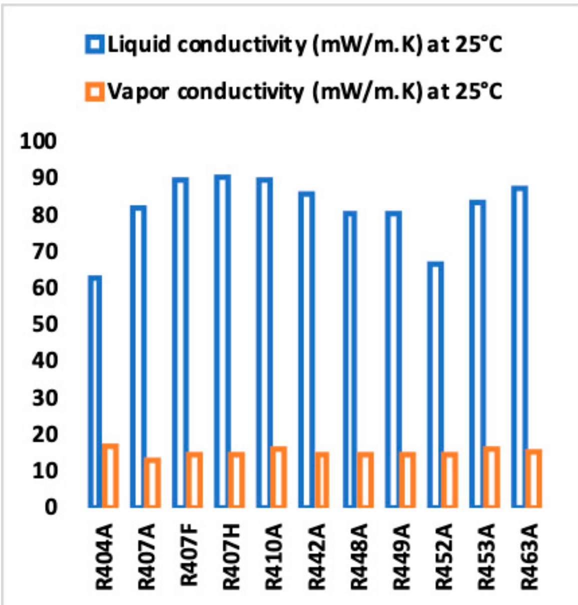

Figure 11. Liquid/vapor conductivity (mW/m.K).

The result of the refrigerant effect in Figure 12 shows that R463A has the highest refrigerant effect, at 194.65, 186.07, and 168.25 kJ/kg for low, medium, and high conditions, respectively. This is 57% and 25% higher for low and medium conditions, respectively, compared to R404A. The result of heat rejection, shown in Figure 13, indicates that the maximal heat-rejection values for R463A were 340.43, 273.5, and 239.3 kJ/kg for the low, medium, and high conditions, respectively, which were 53% and 27% higher for the low and medium conditions, respectively, compared to those of R404A. The refrigerant effect and heat rejection of R463A were found to be higher than those of R404A due to the presence of 36% hydrofluorocarbons (HFCs) R32 and 7% carbon dioxide (CO_2) R744 in its composition, which is consistent with R424A [45] and R453A [57], which are composed of hydrocarbons (HCs) at contents of 1.8% and 1.2%, respectively. The mixed-refrigerant design should be comparable to natural refrigerants in terms of having a strong refrigerant effect and high heat rejection.

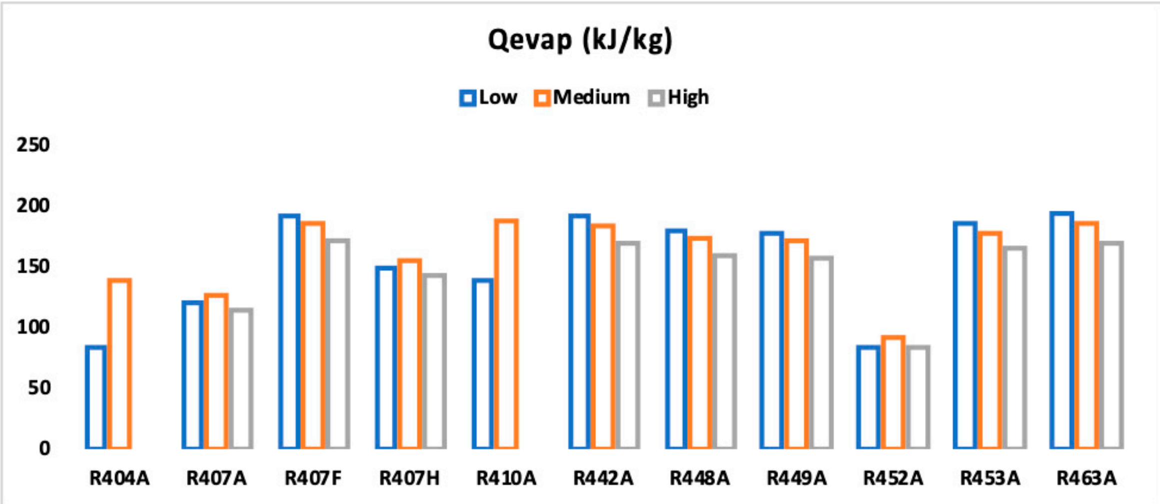

Figure 12. Refrigerant effects of all refrigerants.

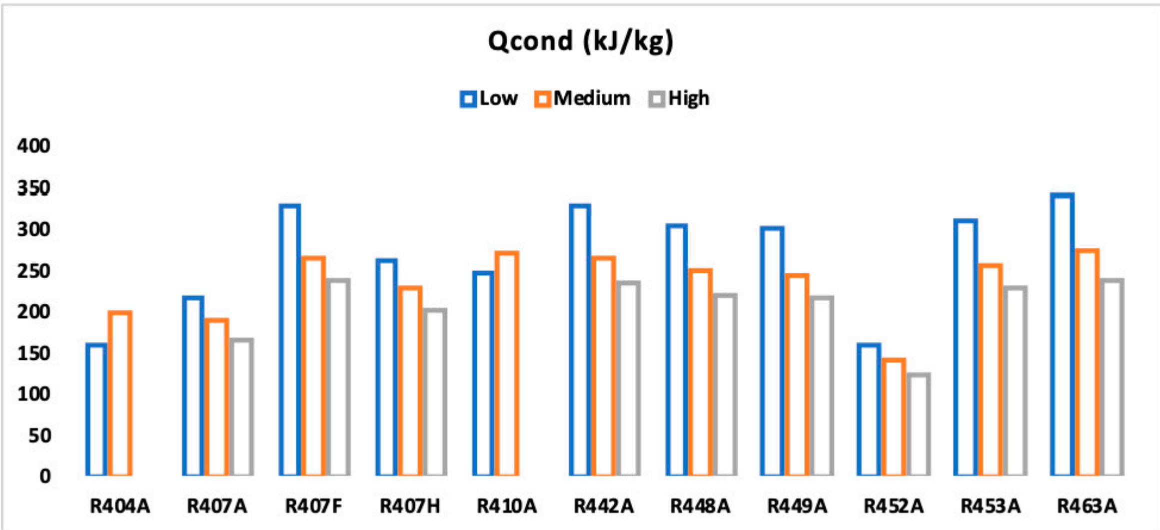

Figure 13. Heat rejection of all refrigerants.

The results of the refrigerant work, shown in Figure 14, demonstrate a relationship between evaporator pressure, shown in Figure 15, and condenser pressure, shown in Figure 16. Refrigerants operated under low pressure display low refrigerant work value; in this case, the lowest refrigerant work of R452A was found to be 75.91, 49.36, and 40.12 kJ/kg for low, medium, and high conditions, respectively. This refrigerant possesses HFOs from R1234yf and R1234ze (E) in its composition. R463A also demonstrated the highest evaporator pressure at 209.1, 554.1, and 934.7 kPa for low, medium and high conditions, respectively, and operated at the highest evaporator pressure of 2748.7, 2988.1, and 3784.7 kPa for low, medium and high conditions, respectively. The highest refrigerant work values for R463A were 145.78, 87.43, and 71.05 kJ/kg, which contained 36% hydrofluorocarbons (HFCs) R32 and 7% carbon dioxide (CO_2) R744, and operated at the highest evaporator pressure of 209.1, 554.1, and 934.7 kPa for low, medium and high conditions, respectively, and operated at the highest evaporator pressure of 2748.7, 2988.1, and 3784.7 kPa for low, medium and high conditions, respectively. This means that a refrigerant system that is operated at low pressure should be mixed with refrigerants that can operate under low pressure, such as R1234yf, R1234ze, and R134A. R450A [49], R456A [50], R513A [51] and R515A [50], which were mixed with hydrofluoroolefins (HFOs) and operated under low pressure, achieving similar results to R463A operating under high pressure with 36% hydrofluorocarbons (HFCs) R32 and 7% carbon dioxide (CO_2) R744 contents in its composition.

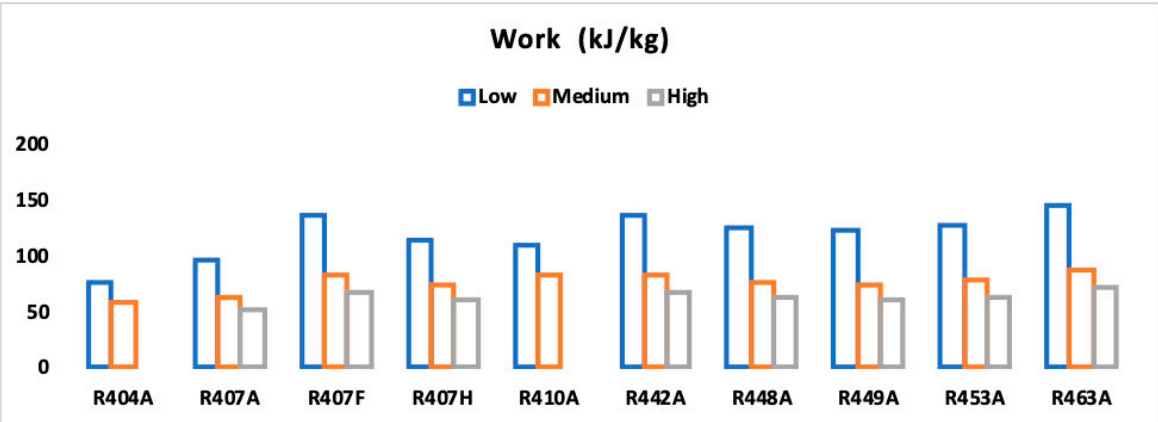

Figure 14. Refrigerant work of all refrigerants.

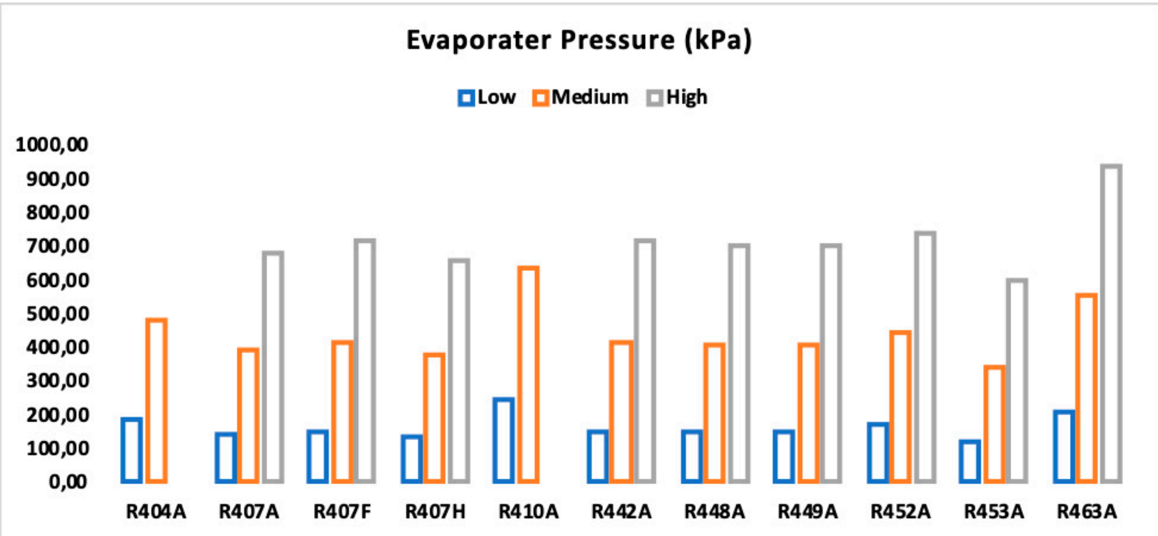

Figure 15. Evaporator pressure of all refrigerants.

The COPc results in Figure 17 show that R453A had the highest COPc at 1.45, 2.3, and 2.607 for low, medium and high conditions, respectively, as R453A did not have the highest refrigerant effect and heat rejection, nor the lowest boiling point, but could be operated under low pressure, which has an impact on low refrigerant work. The COPc level of R463A was recorded at 1.34, which was 10% higher than that of R404A under low-temperature conditions only. The promising results for COPc obtained by R407F, R448A, and R449A were due to the refrigerants being operated under low pressure, which has an impact on low refrigerant work. The same effect was observed for R453A, and these four refrigerants do not have a low normal boiling point or high Cp liquid/vapor or liquid/vapor conductivity. This shows that a mixed-refrigerant design should consider all parameters, such as the GWP, boiling point, Cp liquid/vapor and liquid/vapor conductivity, refrigerant effect, heat rejection, refrigerant work, evaporator pressure, high pressure, and COPc.

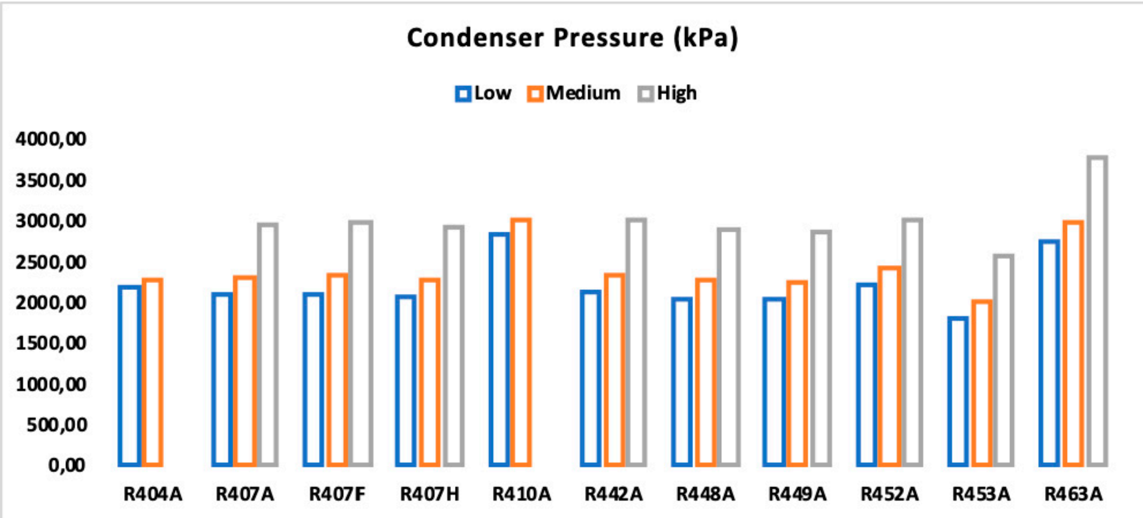

Figure 16. Condenser pressure of all refrigerants.

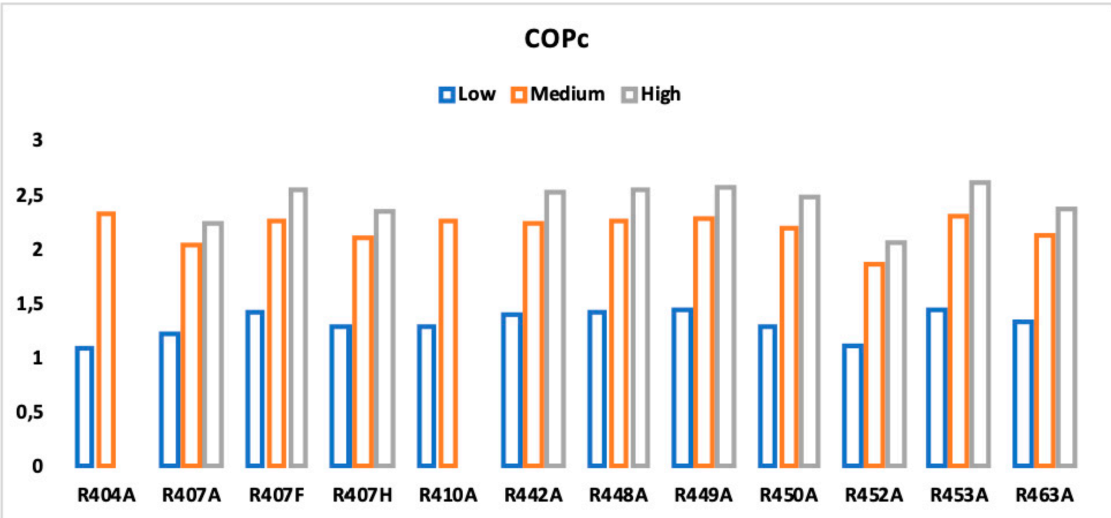

Figure 17. Cooling coefficient of performance (COPc) for all refrigerants.

4. Conclusions

The results for R463A and R404A using REFPROP and CYCLE_D-HX software, and following the CAN/ANSI/AHRI540 AHRI standards, indicate that the normal boiling point of R463A was higher than that of R404A by 23%, with a high cooling capacity and a lower GWP than that of R404A by a margin of 63%. The critical pressure and temperature of R463A were found to be higher than those for R404A; R463A could operate at a higher ambient temperature, has a higher refrigerant effect and heat rejection, and lower global warming potential (GWP) than that of R404A by 52% due to the presence of the HFOs of R1234yf in its composition. The COP of R463A was found to be higher than that of R404A in a low-temperature application. This means that the mixed-refrigerant design should consider all of the parameters, such as the GWP, boiling point, Cp liquid/vapor and liquid/vapor conductivity, refrigerant effect, heat rejection, refrigerant work, evaporator pressure, high pressure, and COPc. R463A is another alternate refrigerant option that is composed of 7% carbon dioxide (CO_2), and is consistent with the evolution of the fourth-generation refrigerants that contain a mixture of HFCs, HFOs, HCs, and natural refrigerants, which are required to produce a low-GWP, zero-ODP, high-capacity, low-operating-pressure, and nontoxic refrigerant. In the future, researchers should incorporate R744 at contents above 7% in order to use natural refrigerants that are low-cost. The problems of high evaporator pressure and high condenser pressure that impact high refrigerant work can be solved by adjusting the composition of the refrigerant or mix using a refrigerant that operates at low pressure, thereby improving the COP of the refrigerant.

Author Contributions: Conceptualization; Software; Validation; Formal Analysis; Investigation; Resources; Data Curation; Writing-Original Draft Preparation; Writing-Review & Editing, P.S.; Visualization; Supervision; Project Administration; Funding Acquisition, J.T., K.M., S.S.-u. and T.T. All authors have read and agreed to the published version of the manuscript.

Funding: This research was funded by Prince of Songkla University and SANYO S.M.I. (Thailand) Co., Ltd.

Acknowledgments: This study was supported by SANYO S.M.I. (Thailand) Co., Ltd. and Buranin Industry Co., Ltd.

Conflicts of Interest: The authors declare no conflict of interest.

References

1. Jeffrey Kuo, C.-F.; Lin, C.-H.; Lee, M.-H. Analyze the energy consumption characteristics and affecting factors of Taiwan's convenience stores-using the big data mining approach. *Energy Build.* **2018**, *168*, 120–136. [CrossRef]
2. Shen, H.; Xu, K.; Freihaut, J. A statistical study on energy performance of U.S. convenience stores: Investigation of factors and bench marking on store energy use. *Energy Build.* **2019**, *183*, 792–802. [CrossRef]
3. Tassou, S.A.; Ge, Y.; Hadawey, A.; Marriott, D. Energy consumption and conservation in food retailing. *Appl. Therm. Eng.* **2011**, *31*, 147–156. [CrossRef]
4. Wang, A.-P.; Hsu, P.-L. The network-based energy management system for convenience stores. *Energy Build.* **2008**, *40*, 1437–1445. [CrossRef]
5. Chou, D.-C.; Chang, C.-S.; Hsu, Y.-Z. Investigation and analysis of power consumption in convenience stores in Taiwan. *Energy Build.* **2016**, *133*, 670–687. [CrossRef]
6. Evans, J.A.; Hammond, E.C.; Gigiel, A.J.; Fostera, A.M.; Reinholdt, L.; Fikiin, K.; Zilio, C. Assessment of methods to reduce the energy consumption of food cold stores. *Appl. Therm. Eng.* **2014**, *62*, 697–705. [CrossRef]
7. Arora, P.; Tyagi, A.; Seshadri, G. Fourth Generation Refrigerant: HFO 1234 yf. *Biology* **2018**, *115*, 1497. [CrossRef]
8. Mota-Babiloni, A.; Navarro-Esbrí, J.; Makhnatch, P.; Molés, F. Refrigerant R32 as lower GWP working fluid in residential air conditioning systems in Europe and the USA. *Renew. Sustain. Energy Rev.* **2017**, *80*, 1031–1042. [CrossRef]
9. Cardoso, B.J.; Lamas, F.B.; Gaspar, A.R.; Ribeiro, J.B. Refrigerants used in the Portuguese food industry: Current status. *Int. J. Refrig.* **2017**, *83*, 60–74. [CrossRef]
10. Sánchez, D.; Cabello, R.; Llopis, R.; Catalán-Gil, J.; Nebot-Andrés, L. Energy assessment and environmental impact analysis of an R134a/R744 cascade refrigeration plant upgraded with the low-GWP refrigerants R152a, R1234ze(E), propane (R290) and propylene (R1270). *Int. J. Refrig.* **2019**, *104*, 321–334. [CrossRef]
11. Calleja-Anta, D.; Nebot-Andrés, L.; Catalán-Gil, J.; Sánchez, D.; Cabello, R.; Llopis, R. Thermodynamic screening of alternative refrigerants for R290 and R600a. *Results Eng.* **2020**, *5*, 100081. [CrossRef]
12. Massuchetto, L.H.P.; Nascimento, R.B.C.d.; Carvalho, S.M.R.d.; Araújo, H.V.d.; d'Angelo, J.V.H. Thermodynamic performance evaluation of a cascade refrigeration system with mixed refrigerants: R744/R1270, R744/R717 and R744/RE170. *Int. J. Refrig.* **2019**, *106*, 201–212. [CrossRef]
13. Zhang, L.; Yang, C.; Liu, H.; Du, P.; Gao, H. Theoretical Investigation on the Properties of R744/R290 Mixtures. *Procedia Eng.* **2017**, *205*, 1620–1626. [CrossRef]
14. Mečárik, K.; Masaryk, M. Thermodynamic properties of refrigerants R11, R12, R13, R14, R22, R23, R113, R114, R500 and R502. *Heat Recovery Syst. CHP* **1991**, *11*, 193–197. [CrossRef]

15. Bao, Z.Y.; Fletcher, D.F.; Haynes, B.S. Flow boiling heat transfer of Freon R11 and HCFC123 in narrow passages. *Int. J. Heat Mass Transf.* **2000**, *43*, 3347–3358. [CrossRef]
16. Chen, S.; Liu, J.; Liu, X.; Hou, Y. An experimental comparison of heat transfer characteristic between R134-a and R22 in spray cooling. *Exp. Therm. Fluid Sci.* **2015**, *66*, 206–212. [CrossRef]
17. Fatouh, M.; Ibrahim, T.A.; Mostafa, A. Performance assessment of a direct expansion air conditioner working with R407C as an R22 alternative. *Appl. Therm. Eng.* **2010**, *30*, 127–133. [CrossRef]
18. Kuczynski, W.; Bohdal, T.; Meyer, J.P.; Denis, A. A regressive model for dynamic instabilities during the condensation of R404A and R507 refrigerants. *Int. J. Heat Mass Transf.* **2019**, *141*, 1025–1035. [CrossRef]
19. Kuczynski, W. Experimental research on condensation of R134a and R404A refrigerants in mini-channels during impulsive instabilities. Part I. *Int. J. Heat Mass Transf.* **2019**, *128*, 728–738. [CrossRef]
20. Kondou, C.; Umemoto, S.; Koyama, S.; Mitooka, Y. Improving the heat dissipation performance of a looped thermosyphon using low-GWP volatile fluids R1234ze(Z) and R1234ze(E) with a super-hydrophilic boiling surface. *Appl. Therm. Eng.* **2017**, *118*, 147–158. [CrossRef]
21. Colombo, L.P.M.; Lucchini, A.; Molinaroli, L. Experimental analysis of the use of R1234yf and R1234ze(E) as drop-in alternatives of R134a in a water-to-water heat pump. *Int. J. Refrig.* **2020**. [CrossRef]
22. Sun, Z.; Cui, Q.; Wang, Q.; Ning, J.; Guo, J.; Dai, B.; Liu, Y.; Xu, Y. Experimental study on CO_2/R32 blends in a water-to-water heat pump system. *Appl. Therm. Eng.* **2019**, *162*, 114303. [CrossRef]
23. Hu, X.; Yang, T.; Meng, X.; Wu, J. Isothermal vapor liquid equilibrium measurements for difluoromethane (R32) + fluoroethane (R161) + trans-1,3,3,3-tetrafluoropropene (R1234ze(E)) ternary mixtures. *Int. J. Refrig.* **2017**, *79*, 49–56. [CrossRef]
24. Ju, F.; Fan, X.; Chen, Y.; Zhang, H.; Wang, T.; Tang, X. Performance assessment of heat pump water heaters with R1233zd(E)/HCs binary mixtures. *Appl. Therm. Eng.* **2017**, *123*, 1345–1355. [CrossRef]
25. Longo, G.A.; Mancin, S.; Righetti, G.; Zilio, C.; Steven Brown, J. Assessment of the low-GWP refrigerants R600a, R1234ze(Z) and R1233zd(E) for heat pump and organic Rankine cycle applications. *Appl. Therm. Eng.* **2020**, *167*, 114804. [CrossRef]
26. Zhang, Y.; He, Y.; Wang, Y.; Wu, X.; Jia, M.; Gong, Y. Experimental Investigation of the Performance of an R1270/CO_2 Cascade Refrigerant System. *Int. J. Refrig.* **2020**. [CrossRef]
27. Zhang, Y.; Wang, X.; Yin, J. Viscosity of saturated mixtures of 1-hexyl-3-methyl-imidazolium bis(trifluoromethylsulfonyl)amide with R600a and R152a. *J. Chem. Thermodyn.* **2020**, *141*, 105970. [CrossRef]
28. Longo, G.A.; Righetti, G.; Zilio, C. Heat-transfer assessment of the low GWP substitutes for traditional HFC refrigerants. *Int. J. Heat Mass Transf.* **2019**, *139*, 31–38. [CrossRef]
29. Shaik, S.V.; Babu, T.P.A. Theoretical Computation of Performance of Sustainable Energy Efficient R22 Alternatives for Residential Air Conditioners. *Energy Procedia* **2017**, *138*, 710–716. [CrossRef]
30. La Rocca, V.; Panno, G. Experimental performance evaluation of a vapour compression refrigerating plant when replacing R22 with alternative refrigerants. *Appl. Energy* **2011**, *88*, 2809–2815. [CrossRef]
31. Kasera, S.; Bhaduri, S.C. Performance of R407C as an Alternate to R22: A Review. *Energy Procedia* **2017**, *109*, 4–10. [CrossRef]
32. Elgendy, E.; Melike, M.; Fatouh, M. Experimental assessment of a split air conditioner working with R-417A under different indoor and outdoor conditions. *Int. J. Refrig.* **2018**, *85*, 268–281. [CrossRef]
33. Fernández-Seara, J.; Uhía, F.J.; Diz, R.; Dopazo, J.A. Vapour condensation of R22 retrofit substitutes R417A, R422A and R422D on CuNi turbo C tubes. *Int. J. Refrig.* **2010**, *33*, 148–157. [CrossRef]
34. Aprea, C.; Maiorino, A. An experimental investigation of the global environmental impact of the R22 retrofit with R422D. *Energy* **2011**, *36*, 1161–1170. [CrossRef]
35. Oruç, V.; Devecioğlu, A.G. Thermodynamic performance of air conditioners working with R417A and R424A as alternatives to R22. *Int. J. Refrig.* **2015**, *55*, 120–128. [CrossRef]
36. Chen, X.; Liu, C.; Yang, J.; Chen, J. Experimental study on R-22, R-427A, R-161 and R-290 in air-source heat pump for space heating at low ambient temperatures. *Int. J. Refrig.* **2018**, *96*, 147–154. [CrossRef]
37. Devecioğlu, A.G.; Oruç, V. The influence of plate-type heat exchanger on energy efficiency and environmental effects of the air-conditioners using R453A as a substitute for R22. *Appl. Therm. Eng.* **2017**, *112*, 1364–1372. [CrossRef]
38. Yang, M.; Zhang, H.; Meng, Z.; Qin, Y. Experimental study on R1234yf/R134a mixture (R513A) as R134a replacement in a domestic refrigerator. *Appl. Therm. Eng.* **2019**, *146*, 540–547. [CrossRef]

39. Makhnatch, P.; Mota-Babiloni, A.; López-Belchí, A.; Khodabandeh, R. R450A and R513A as lower GWP mixtures for high ambient temperature countries: Experimental comparison with R134a. *Energy* **2019**, *166*, 223–235. [CrossRef]
40. Heredia-Aricapa, Y.; Belman-Flores, J.M.; Mota-Babiloni, A.; Serrano-Arellano, J.; García-Pabón, J.J. Overview of low GWP mixtures for the replacement of HFC refrigerants: R134a, R404A and R410A. *Int. J. Refrig.* **2020**, *111*, 113–123. [CrossRef]
41. López-Belchí, A. Assessment of a mini-channel condenser at high ambient temperatures based on experimental measurements working with R134a, R513A and R1234yf. *Appl. Therm. Eng.* **2019**, *155*, 341–353. [CrossRef]
42. Mota-Babiloni, A.; Navarro-Esbrí, J.; Peris, B.; Molés, F.; Verdú, G. Experimental evaluation of R448A as R404A lower-GWP alternative in refrigeration systems. *Energy Convers. Manag.* **2015**, *105*, 756–762. [CrossRef]
43. Hu, X.; Zhang, Z.; Yao, Y.; Wang, Q. Non-azeotropic refrigerant charge optimization for cold storage unit based on year-round performance evaluation. *Appl. Therm. Eng.* **2018**, *139*, 395–401. [CrossRef]
44. Bortolini, M.; Gamberi, M.; Gamberini, R.; Graziani, A.; Lolli, F.; Regattieri, A. Retrofitting of R404a commercial refrigeration systems using R410a and R407f refrigerants. *Int. J. Refrig.* **2015**, *55*, 142–152. [CrossRef]
45. Mota-Babiloni, A.; Makhnatch, P.; Khodabandeh, R. Recent investigations in HFCs substitution with lower GWP synthetic alternatives: Focus on energetic performance and environmental impact. *Int. J. Refrig.* **2017**, *82*, 288–301. [CrossRef]
46. Mancin, S.; Del Col, D.; Rossetto, L. Partial condensation of R407C and R410A refrigerants inside a plate heat exchanger. *Exp. Therm. Fluid Sci.* **2012**, *36*, 149–157. [CrossRef]
47. Oruç, V.; Devecioğlu, A.G.; Ender, S. Improvement of energy parameters using R442A and R453A in a refrigeration system operating with R404A. *Appl. Therm. Eng.* **2018**, *129*, 243–249. [CrossRef]
48. Mendoza-Miranda, J.M.; Mota-Babiloni, A.; Navarro-Esbrí, J. Evaluation of R448A and R450A as low-GWP alternatives for R404A and R134a using a micro-fin tube evaporator model. *Appl. Therm. Eng.* **2016**, *98*, 330–339. [CrossRef]
49. Makhnatch, P.; Mota-Babiloni, A.; Rogstam, J.; Khodabandeh, R. Retrofit of lower GWP alternative R449A into an existing R404A indirect supermarket refrigeration system. *Int. J. Refrig.* **2017**, *76*, 184–192. [CrossRef]
50. Górny, K.; Stachowiak, A.; Tyczewski, P.; Zwierzycki, W. Lubricity of selected oils in mixtures with the refrigerants R452A, R404A, and R600a. *Tribol. Int.* **2019**, *134*, 50–59. [CrossRef]
51. Devecioğlu, A.G.; Oruç, V. An analysis on the comparison of low-GWP refrigerants to alternatively use in mobile air-conditioning systems. *Therm. Sci. Eng. Prog.* **2017**, *1*, 1–5. [CrossRef]
52. Mota-Babiloni, A.; Haro-Ortuño, J.; Navarro-Esbrí, J.; Barragán-Cervera, Á. Experimental drop-in replacement of R404A for warm countries using the low GWP mixtures R454C and R455A. *Int. J. Refrig.* **2018**, *91*, 136–145. [CrossRef]
53. Xu, S.; Fan, X.; Ma, G. Experimental investigation on heating performance of gas-injected scroll compressor using R32, R1234yf and their 20wt%/80wt% mixture under low ambient temperature. *Int. J. Refrig.* **2017**, *75*, 286–292. [CrossRef]
54. Yang, M.-H.; Yeh, R.-H.; Hung, T.-C. Thermo-economic analysis of the transcritical organic Rankine cycle using R1234yf/R32 mixtures as the working fluids for lower-grade waste heat recovery. *Energy* **2017**, *140*, 818–836. [CrossRef]
55. Xu, X.; Hwang, Y.; Radermacher, R. Performance comparison of R410A and R32 in vapor injection cycles. *Int. J. Refrig.* **2013**, *36*, 892–903. [CrossRef]
56. Zhang, X.; Wang, F.; Liu, Z.; Gu, J.; Zhu, F.; Yuan, Q. Performance Research on Heat Pump Using Blends of R744 with Eco-friendly Working Fluid. *Procedia Eng.* **2017**, *205*, 2297–2302. [CrossRef]
57. Longo, G.A.; Mancin, S.; Righetti, G.; Zilio, C. R1234yf and R1234ze(E) as environmentally friendly replacements of R134a: Assessing flow boiling on an experimental basis. *Int. J. Refrig.* **2019**, *108*, 336–346. [CrossRef]
58. Mylona, S.K.; Hughes, T.J.; Saeed, A.A.; Rowland, D.; Park, J.; Tsuji, T.; Tanaka, Y.; Seiki, Y.; May, E.F. Thermal conductivity data for refrigerant mixtures containing R1234yf and R1234ze(E). *J. Chem. Thermodyn.* **2019**, *133*, 135–142. [CrossRef]

59. Tomassetti, S.; Coccia, G.; Pierantozzi, M.; Di Nicola, G.; Brown, J.S. Vapor phase and two-phase PvTz measurements of difluoromethane + 2,3,3,3-tetrafluoroprop-1-ene. *J. Chem. Thermodyn.* **2020**, *141*, 105966. [CrossRef]
60. Fouad, W.A.; Vega, L.F. Transport properties of HFC and HFO based refrigerants using an excess entropy scaling approach. *J. Supercrit. Fluids* **2018**, *131*, 106–116. [CrossRef]
61. Bell, I.H.; Domanski, P.A.; McLinden, M.O.; Linteris, G.T. The hunt for nonflammable refrigerant blends to replace R-134a. *Int. J. Refrig.* **2019**, *104*, 484–495. [CrossRef]
62. Brignoli, R.; Brown, J.S.; Skye, H.M.; Domanski, P.A. Refrigerant performance evaluation including effects of transport properties and optimized heat exchangers. *Int. J. Refrig.* **2017**, *80*, 52–65. [CrossRef] [PubMed]
63. CAN/ANSI/AHRI540. *Performance Rating of Positive Displacement Refrigerant Compressors and Compressor Units*; AHRI: Aiken, SC, USA, 2015; Volume 5.
64. Lumpkin, D.R.; Bahman, A.M.; Groll, E.A. Two-phase injected and vapor-injected compression: Experimental results and mapping correlation for a R-407C scroll compressor. *Int. J. Refrig.* **2018**, *86*, 449–462. [CrossRef]
65. Abas, N.; Kalair, A.R.; Khan, N.; Haider, A.; Saleem, Z.; Saleem, M.S. Natural and synthetic refrigerants, global warming: A review. *Renew. Sustain. Energy Rev.* **2018**, *90*, 557–569. [CrossRef]
66. Zhang, H.; Gao, B.; Li, H.; Zhao, Y.; Wu, W.; Zhong, Q.; Dong, X.; Chen, Y.; Gong, M.; Luo, E. Saturated liquid density equation for pure refrigerants including CFCs, HCFCs, HFCs, HCs, HFOs, HFEs, PFAs and ISs based on the scaling law and the law of rectilinear diameter. *Int. J. Refrig.* **2018**, *87*, 65–77. [CrossRef]
67. Vaghela, J.K. Comparative Evaluation of an Automobile Air—Conditioning System Using R134a and Its Alternative Refrigerants. *Energy Procedia* **2017**, *109*, 153–160. [CrossRef]
68. Llopis, R.; Calleja-Anta, D.; Sánchez, D.; Nebot-Andrés, L.; Catalán-Gil, J.; Cabello, R. R-454C, R-459B, R-457A and R-455A as low-GWP replacements of R-404A: Experimental evaluation and optimization. *Int. J. Refrig.* **2019**, *106*, 133–143. [CrossRef]
69. Wu, X.; Dang, C.; Xu, S.; Hihara, E. State of the art on the flammability of hydrofluoroolefin (HFO) refrigerants. *Int. J. Refrig.* **2019**, *108*, 209–223. [CrossRef]
70. Miyara, A.; Alam, M.J.; Kariya, K. Measurement of viscosity of trans-1-chloro-3,3,3-trifluoropropene (R-1233zd(E)) by tandem capillary tubes method. *Int. J. Refrig.* **2018**, *92*, 86–93. [CrossRef]
71. Domanski, P.A.; Brignoli, R.; Brown, J.S.; Kazakov, A.F.; McLinden, M.O. Low-GWP refrigerants for medium and high-pressure applications. *Int. J. Refrig.* **2017**, *84*, 198–209. [CrossRef] [PubMed]